Hindawi
Journal of Electrical and Computer Engineering
Volume 2021, Article ID 6610107, 9 pages
https://doi.org/10.1155/2021/6610107

Research Article

Performance Analysis for Exact and Upper Bound Capacity in DF Energy Harvesting Full-Duplex with Hybrid TPSR Protocol

Phu Tran Tin,[1] **Phan Van-Duc**,[2] **Tan N. Nguyen**,[3] **and Le Anh Vu**[4]

[1]*Faculty of Electronics Technology, Industrial University of Ho Chi Minh City, Ho Chi Minh City, Vietnam*
[2]*Faculty of Automobile Technology, Van Lang University, Ho Chi Minh City, Vietnam*
[3]*Wireless Communications Research Group, Faculty of Electrical and Electronics Engineering, Ton Duc Thang University, Ho Chi Minh City, Vietnam*
[4]*Optoelectronics Research Group, Faculty of Electrical and Electronics Engineering, Ton Duc Thang University, Ho Chi Minh City, Vietnam*

Correspondence should be addressed to Phan Van-Duc; duc.pv@vlu.edu.vn

Received 2 December 2020; Revised 6 January 2021; Accepted 11 January 2021; Published 27 January 2021

Academic Editor: Jit S. Mandeep

In this paper, we investigate the full-duplex (FD) decode-and-forward (DF) cooperative relaying system, whereas the relay node can harvest energy from radiofrequency (RF) signals of the source and then utilize the harvested energy to transfer the information to the destination. Specifically, a hybrid time-power switching-based relaying method is adopted, which leverages the benefits of time-switching relaying (TSR) and power-splitting relaying (PSR) protocols. While energy harvesting (EH) helps to reduce the limited energy at the relay, full-duplex is one of the most important techniques to enhance the spectrum efficiency by its capacity of transmitting and receiving signals simultaneously. Based on the proposed system model, the performance of the proposed relaying system in terms of the ergodic capacity (EC) is analyzed. Specifically, we derive the exact closed form for upper bound EC by applying some special function mathematics. Then, the Monte Carlo simulations are performed to validate the mathematical analysis and numerical results.

1. Introduction

In the last few decades, energy harvesting (EH) has received significant attention from the researchers [1–10]. By recharging energy from surrounding sources such as solar [2], thermoelectric, wind, and radiofrequency (RF) signals, relay users can perform information forwarding without depending on external sources or battery replacement. Particularly, the RF-based EH gains great interest because it can bring energy and data simultaneously. Varshney first introduced the concept of simultaneous wireless information and power transfer (SWIPT) [1]. Then, Grover and Sahai [7] continued Varshney's work by studying the frequency-selective channel. Then, two practical SWIPT designs termed the time switching (TS) and power splitting (PS) are proposed and studied in [5]. In the TS method, the receiver can divide the total transmission time into two portions: the first one is utilized for EH, and the second one is reserved for the data reception process. In the PS method, a portion of received RF power is used for EH, and then, the rest is utilized for decoding signals.

Based on TS and PS architectures in [5], Nasir et al. [9] proposed two relaying schemes, termed the TS-based relaying (TSR) and PS-based relaying (PSR), to enable EH and information decoding at the relay node. Many works have been done to study TSR [4, 6, 10], PSR [3], and both TSR and PSR [8]. In [4], the authors investigated the secrecy performance of multihop multipath wireless sensor networks (WSNs) under the impact of EH and hardware impairment. Specifically, each relay node harvested energy from the power beacon (PB) by using TSR and then used this energy to forward the information to the next receiver. Hieu et al. in [6] studied the throughput maximization in backscatter- and cache-assisted UAV communications. Herein, a UAV was

replenished by RF signals from the source, and then, it used this energy to backscatter information to the destination. Moreover, both linear EH and nonlinear EH models were considered in this work. The authors in [10] solved energy limitation and spectrum constraints for cognitive radio WSNs, whereas the secondary source and relay users were able to harvest energy from a multiantenna PB. In contrast to [4, 6, 10] that studied TSR, Tin et al. [3] considered PSR. Specifically, the authors investigated the secrecy performance of the FD PB-aided EH relaying cooperative network. Moreover, they derived the exact closed form of outage probability (OP) and system throughput (ST) under PSR protocol. In [8], Sumit et al. proposed a novel hybrid backscatter and relaying scheme to leverage SWIPT considering both TSR and PSR methods in 6G green IoT networks.

Despite remarkable achievements, TSR and PSR have their own drawbacks. For instance, the TSR method outperforms the PSR method at low SNR, and the PSR obtains better performance at high SNR. This is the motivation for a new approach, namely, the hybrid time-power switching relaying (TPSR) method [11–14]. Tan et al. [11] studied the performance of a two-way amplify-and-forward (AF) EH cooperative network over Rician fading channels. Specifically, the closed-form results of the achievable throughput, outage probability (OP), ergodic capacity (EC), and symbol error rate (SER) for the DL and DT transmission modes are derived. Saman et al. [12] aimed at maximizing the total throughput from source to destination for both DF and AF schemes by optimizing the TS and PS ratios at the relay. Tin et al. [13] investigated EH two-way half-duplex (TWHD) relaying WSN adopting selection combining (SC) over block Rayleigh fading channel. In particular, the direct link between source and destination was also considered to enhance network performance.

Besides, the EH technique reduces the limited energy at the relay, and full-duplex is one of the essential techniques to enhance the spectrum efficiency by transmitting and receiving signals simultaneously. Motivated by the above discussion, this paper proposed and investigated the system performance analysis of the full-duplex (FD) DF relaying system, in which the relay node can harvest energy from RF signals of the source and then utilize the harvested energy to transfer the information to the destination. Moreover, the hybrid TPSR protocol is applied to gain the advantages of both TSR and PSR methods. The main contributions of this research are summarized as follows:

(i) A system model of an FD- and EH-assisted DF relaying network with the hybrid TPSR protocol is presented.

(ii) We provide exact and upper bound closed-form expressions of ergodic capacity by adopting a series representation of modified Bessel functions.

(iii) We also show an insightful analysis of the effect of various system parameters on energy and spectrum efficiency.

(iv) The correctness of the mathematical expressions can be validated through the Monte Carlo simulation.

The remaining of this paper is organized as follows. In Section 2, the system model of the FD- and EH-assisted DF relay network is described in detail. Then, in Section 3, we provide the ergodic capacity analysis of the system. Section 4 derives the closed form of the upper bound EC. Numerical results to support our analysis are presented in Section 5. Finally, Section 5 concludes the paper.

2. System Model

We consider an FD- and EH-assisted DF relaying network as in Figure 1, where a relay R helps to forward data from a source to a destination. Moreover, the direct transmission link from source S to destination D is missing due to severe fading or heavy obstacles. Besides, the source and destination are single-antenna devices and operates on half-duplex mode. The relay node is equipped with two antennas and works on the FD mode. Since the relay is able to transmit and receive the signal simultaneously, there exists residual interference h_{RR} at the relay R. As displayed in Figure 2, the total transmission time T is divided into two parts. In the first fraction of time, αT, the relay node is harvest energy from source S, where $0 \le \alpha \le 1$ is the time-switching factor. In the rest time, $(1-\alpha)T$, the PSR is applied. Specifically, a portion of power ρP_S is used for EH, and the second part $(1-\rho)P_S$ is used for information decoding, with $0 \le \rho \le 1$ is the power-splitting factor. Moreover, we assume that the transmission channels between two arbitrary users are block Rayleigh fading, where channel coefficients are unchanged during one transmission block and vary independently across different blocks.

As above, we assumed that all of the channels are Rayleigh fading. Hence, the channel gains $|h_{\mathrm{SR}}|^2$, $|h_{\mathrm{RD}}|^2$ are exponential random variables (RVs) whose CDF are given as

$$\begin{aligned} F_{|h_{\mathrm{SR}}|^2}(x) &= 1 - \exp\left(-\lambda_{\mathrm{SR}} x\right), \\ F_{|h_{\mathrm{RD}}|^2}(x) &= 1 - \exp\left(-\lambda_{\mathrm{RD}} x\right). \end{aligned} \tag{1}$$

To take path-loss into account, we can model the parameters as follows:

$$\begin{aligned} \lambda_{\mathrm{SR}} &= \left(d_{\mathrm{SR}}\right)^{\chi}, \\ \lambda_{\mathrm{RD}} &= \left(d_{\mathrm{RD}}\right)^{\chi}, \end{aligned} \tag{2}$$

where χ denotes the path-loss exponent and d_{SR} and d_{SD} are link distances of the $\mathrm{S} \longrightarrow \mathrm{R}$ and $\mathrm{R} \longrightarrow \mathrm{D}$ links, respectively.

The RV h_{RR} is also modeled as a complex Gaussian RV, and hence, $|h_{\mathrm{RR}}|^2$ is also an exponential RV, whose CDF is expressed as

$$F_{|h_{\mathrm{RR}}|^2}(x) = 1 - \exp\left(-\lambda_{\mathrm{RR}} x\right). \tag{3}$$

Then, the PDFs of $|h_{\mathrm{SR}}|^2$, $|h_{\mathrm{RD}}|^2$, and $|h_{\mathrm{RR}}|^2$ are expressed, respectively, as

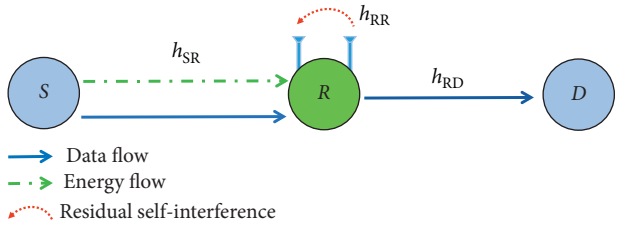

Figure 1: System model.

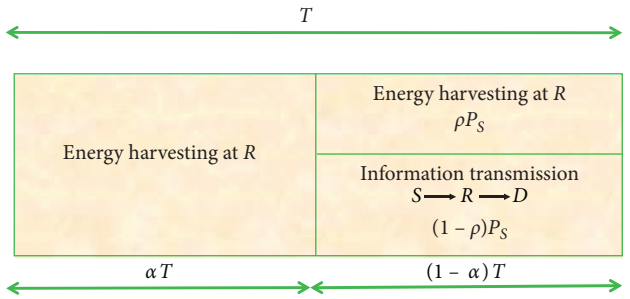

Figure 2: IT and EH processes with hybrid time-power-splitting relaying protocols.

$$f_{|h_{SR}|^2}(x) = \lambda_{SR}\exp(-\lambda_{SR}x),$$
$$f_{|h_{RD}|^2}(x) = \lambda_{RD}\exp(-\lambda_{RD}x), \quad (4)$$
$$f_{|h_{RR}|^2}(x) = \lambda_{RR}\exp(-\lambda_{RR}x).$$

The received signal at the relay can be expressed as

$$y_R = \sqrt{1-\rho}h_{SR}x_s + h_{RR}x_R + n_R, \quad (5)$$

where $x_s$is the energy symbol with $E\{|x_s|^2\} = P_s$, x_s is the loopback interference due to full-duplex relaying and satisfies $E\{|x_R|^2\} = P_R$, in which E{•} denotes the expectation operation, n_R is the zero-mean additive white Gaussian noise (AWGN) with variance N_0, and h_{RR} is the residual self-interference channel.

At the first and second time slot, the harvested energy at the relay can be computed as

$$E_R^1 = \eta\alpha T P_s|h_{SR}|^2,$$
$$E_R^2 = \eta(1-\alpha)\rho T P_s|h_{SR}|^2. \quad (6)$$

From (6), the amount average transmit power of the relay node can be obtained as

$$P_R = \frac{E_R^1 + E_R^2}{(1-\alpha)T} = \frac{\eta\alpha P_s|h_{SR}|^2}{(1-\alpha)} + \eta\rho P_s|h_{SR}|^2 = \kappa P_s|h_{SR}|^2, \quad (7)$$

where $0 \le \eta \le 1$ denotes the energy conversion efficiency, which takes into account the energy loss by harvesting decoding and processing circuits and $\kappa = \eta\alpha/1-\alpha+\eta\rho$.

The received signal at the destination can be given as

$$y_D = h_{RD}x_R + n_D, \quad (8)$$

where n_D is the AWGN with variance N_0.

In our model, we adopt the decode-and-forward (DF) protocol. Hence, the signal to interference noise (SINR) at the relay node from (5) can be given as

$$\gamma_R = \frac{(1-\rho)P_s|h_{SR}|^2}{|h_{RR}|^2 P_R + N_0}. \quad (9)$$

Substituting (7) into (9) and using the fact that $N_0 << P_S$, we have

$$\gamma_R = \frac{(1-\rho)P_s|h_{SR}|^2}{\kappa P_s|h_{SR}|^2|h_{RR}|^2 + N_0} \approx \frac{1-\rho}{\kappa|f|^2}. \quad (10)$$

From (8), the SINR at the destination can be obtained as

$$\gamma_D = \frac{|h_{RD}|^2 P_R}{N_0} = \frac{\kappa P_s|h_{SR}|^2|h_{RD}|^2}{N_0} = \kappa\Psi|h_{SR}|^2|h_{RD}|^2, \quad (11)$$

where $\Psi = P_s/N_0$.

Finally, the overall SINR of the system in DF mode can be claimed as follows [15–18]:

$$\gamma_{DF} = \min(\gamma_R, \gamma_D) = \min\left(\frac{1-\rho}{\kappa|h_{RR}|^2}, \kappa\Psi|h_{SR}|^2|h_{RD}|^2\right) = \min\left(\frac{1-\rho}{\kappa Z}, \kappa\Psi XY\right), \quad (12)$$

where $X = |h_{SR}|^2, Y = |h_{RD}|^2, Z = |h_{RR}|^2$.

3. Ergodic Capacity (EC) Analysis

The EC of the system can be defined as follows [1]:

$$EC = \frac{1}{\ln 2}\int_0^{\infty}\frac{1-F_{\gamma_{DF}}(x)}{1+x}\mathrm{d}x. \tag{13}$$

To find the integral in (13), we first find the CDF of γ_{DF} calculated as

$$F_{\gamma_{DF}}(x) = \Pr(\gamma_{DF} < x) = \Pr\left(\min\left(\frac{1-\rho}{\kappa Z}, \kappa\Psi XY\right) < x\right) = 1 - \underbrace{\Pr\left(\frac{1-\rho}{\kappa Z} \geq x\right)}_{P_1}\underbrace{\Pr(\kappa\Psi XY \geq x)}_{P_2}. \tag{14}$$

From (14), P_1 can be calculated as

$$P_1 = \Pr\left(\frac{1-\rho}{\kappa Z} \geq x\right) = \Pr\left(Z \leq \frac{1-\rho}{\kappa x}\right) = 1 - \exp\left(-\frac{\lambda_{RR}(1-\rho)}{\kappa x}\right). \tag{15}$$

Next, P_2 can be computed as

$$\begin{aligned} P_2 &= \Pr(\kappa\Psi XY \geq x) = 1 - \Pr(\kappa\Psi XY < x) = 1 - \Pr\left(X < \frac{x}{\kappa\Psi Y}\right) \\ &= 1 - \int_0^{\infty} F_X\left(\frac{x}{\kappa\Psi y}|Y = y\right) f_Y(y)\mathrm{d}y = \int_0^{\infty}\lambda_{RD}\exp\left(-\frac{\lambda_{SR}x}{\kappa\Psi y} - \lambda_{RD}y\right)\mathrm{d}y. \end{aligned} \tag{16}$$

By applying eq [3.324,1] (14), P_2 can be rewritten as

$$P_2 = 2\sqrt{\frac{\lambda_{SR}\lambda_{RD}x}{\kappa\Psi}} \times K_1\left(2\sqrt{\frac{\lambda_{SR}\lambda_{RD}x}{\kappa\Psi}}\right), \tag{17}$$

where $K_v(\bullet)$ is the modified Bessel function of the second kind and v-th order. Substituting (16) and (17) into (14), we have

$$F_{\gamma_{DF}}(x) = 1 - 2\left\{1 - \exp\left(-\frac{\lambda_{RR}(1-\rho)}{\kappa x}\right)\right\} \times \sqrt{\frac{\lambda_{SR}\lambda_{RD}x}{\kappa\Psi}} \times K_1\left(2\sqrt{\frac{\lambda_{SR}\lambda_{RD}x}{\kappa\Psi}}\right). \tag{18}$$

Finally, by substituting (18) into (13), the exact EC can be obtained as

$$EC = \frac{2}{\ln 2}\int_0^{\infty}\frac{\{1-\exp(-\lambda_{RR}(1-\rho)/\kappa x)\} \times \sqrt{\lambda_{SR}\lambda_{RD}x/\kappa\Psi} \times K_1\left(2\sqrt{\lambda_{SR}\lambda_{RD}x/\kappa\Psi}\right)}{1+x}\mathrm{d}x. \tag{19}$$

4. Upper Bound EC Analysis

To the best of our knowledge, the (19) integration has no closed-form result. Therefore, in this section, we try to find the different EC analyses in upper bound form. The upper bound EC can be defined as follows [2]:

$$EC_{\mathrm{UP}} = \log_2\left(1 + \mathrm{E}\{\gamma_{\mathrm{DF}}\}\right), \tag{20}$$

where

$$\mathrm{E}\{\gamma_{\mathrm{DF}}\} = \int_0^{\infty} x \times f_{\gamma_{\mathrm{DF}}}(x)\mathrm{d}x. \tag{21}$$

From (18), $f_{\gamma_{\mathrm{DF}}}(x)$ can be found as

$$\begin{aligned} f_{\gamma_{\mathrm{DF}}}(x) = \frac{\partial F_{\gamma_{\mathrm{DF}}}(x)}{\partial x} &= \frac{2\lambda_{\mathrm{RR}}(1-\rho)}{\kappa x^2}\exp\left(-\frac{\lambda_{\mathrm{RR}}(1-\rho)}{\kappa x}\right)\sqrt{\frac{\lambda_{\mathrm{SR}}\lambda_{\mathrm{RD}}x}{\kappa\Psi}} \times K_1\left(2\sqrt{\frac{\lambda_{\mathrm{SR}}\lambda_{\mathrm{RD}}x}{\kappa\Psi}}\right) \\ &+ \frac{2\lambda_{SR}\lambda_{RD}}{\kappa\Psi}\left\{1 - \exp\left(-\frac{\lambda_{\mathrm{RR}}(1-\rho)}{\kappa x}\right)\right\} \times K_0\left(2\sqrt{\frac{\lambda_{\mathrm{SR}}\lambda_{\mathrm{RD}}x}{\kappa\Psi}}\right). \end{aligned} \tag{22}$$

Substituting (22) into (21), we can claim as

$$\mathrm{E}\{\gamma_{\mathrm{DF}}\} = \Xi_1 + \Xi_2, \tag{23}$$

where

$$\Xi_1 = \frac{2\lambda_{\mathrm{RR}}(1-\rho)}{\kappa} \times \int_0^{\infty} \sqrt{\frac{\Theta_3}{x}} \times \exp(-\Theta_4) \times K_1\left(2\sqrt{\Theta_3}\right)\mathrm{d}x. \tag{24}$$

By changing variable $t = \kappa\Psi/\lambda_{\mathrm{SR}}\lambda_{\mathrm{RD}}x$, equation (24) can be reformulated by

$$\Xi_1 = \frac{2\lambda_{\mathrm{RR}}(1-\rho)}{\kappa} \times \int_0^{\infty} t^{-3/2} \times xp\left(-\frac{\lambda_{\mathrm{SR}}\lambda_{\mathrm{RD}}\lambda_{\mathrm{RR}}(1-\rho)t}{\kappa^2\Psi}\right) \times K_1\left(\frac{2}{\sqrt{t}}\right)\mathrm{d}t. \tag{25}$$

By using the same proof as [3], equation (25) can be rewritten by

$$\Xi_1 = \frac{\lambda_{\mathrm{RR}}(1-\rho)}{\kappa^2}\sqrt{\frac{\lambda_{\mathrm{SR}}\lambda_{\mathrm{RD}}\lambda_{\mathrm{RR}}(1-\rho)}{\Psi}} \times G_{0,3}^{3,0}\left(\frac{\lambda_{\mathrm{SR}}\lambda_{\mathrm{RD}}\lambda_{\mathrm{RR}}(1-\rho)}{\kappa^2\Psi}\middle|\frac{-1}{2}, \frac{-1}{2}, \frac{1}{2}\right), \tag{26}$$

where $G_{p,q}^{m,n}\left(z\middle|\begin{matrix}a_1,\ldots,a_p\\ b_1,\ldots,b_q\end{matrix}\right)$ is the Meijer G function.

Next, Ξ_2 can be calculated as

$$\begin{aligned} \Xi_2 &= \int_0^{\infty} 2\frac{\lambda_{\mathrm{SR}}\lambda_{\mathrm{RD}}x}{\kappa\Psi}\left\{1 - \exp\left(-\frac{\lambda_{\mathrm{RR}}(1-\rho)}{\kappa x}\right)\right\} \times K_0\left(2\sqrt{\frac{\lambda_{\mathrm{SR}}\lambda_{\mathrm{RD}}x}{\kappa\Psi}}\right)\mathrm{d}x \\ &= \underbrace{\int_0^{\infty} 2\frac{\lambda_{\mathrm{SR}}\lambda_{\mathrm{RD}}x}{\kappa\Psi} \times K_0\left(2\sqrt{\frac{\lambda_{\mathrm{SR}}\lambda_{\mathrm{RD}}x}{\kappa\Psi}}\right)\mathrm{d}x}_{\Xi_{2,1}} - \underbrace{\int_0^{\infty} 2\frac{\lambda_{\mathrm{SR}}\lambda_{\mathrm{RD}}x}{\kappa\Psi} \times \exp\left(-\frac{\lambda_{\mathrm{RR}}(1-\rho)}{\kappa x}\right) \times K_0\left(2\sqrt{\frac{\lambda_{\mathrm{SR}}\lambda_{\mathrm{RD}}x}{\kappa\Psi}}\right)\mathrm{d}x}_{\Xi_{2,2}}. \end{aligned} \tag{27}$$

By adopting $y = \sqrt{\lambda_{SR}\lambda_{RD}x/\kappa\Psi}$, $\Xi_{2,1}$ can be reformulated as

$$\begin{aligned}\Xi_2 &= \int_0^\infty \frac{2\lambda_{SR}\lambda_{RD}x}{\kappa\Psi}\left\{1-\exp\left(-\frac{\lambda_{RR}(1-\rho)}{\kappa x}\right)\right\}\times K_0\left(2\sqrt{\frac{\lambda_{SR}\lambda_{RD}x}{\kappa\Psi}}\right)dx \\ &= \underbrace{\int_0^\infty 2\Theta_3 \times K_0\left(2\sqrt{\frac{\lambda_{SR}\lambda_{RD}x}{\kappa\Psi}}\right)dx}_{\Xi_{2,1}} - \underbrace{\int_0^\infty \frac{2\lambda_{SR}\lambda_{RD}x}{\kappa\Psi}\times \exp\left(-\frac{\lambda_{RR}(1-\rho)}{\kappa x}\right)dx}_{\Xi_{2,2}}.\end{aligned} \tag{28}$$

With the help of eq [6.561,14] in (14), we obtain

$$\Xi_{2,1} = \frac{\kappa\Psi}{\lambda_{SR}\lambda_{RD}}. \tag{29}$$

The same proof for $\Xi_{2,2}$ is as above, and we can claim as follows:

$$\begin{aligned}\Xi_{2,2} &= \frac{2\kappa\Psi}{\lambda_{SR}\lambda_{RD}}\int_0^\infty t^{-3}\times \exp\left(-\frac{\lambda_{SR}\lambda_{RD}\lambda_{RR}(1-\rho)t}{\kappa^2\Psi}\right)K_0\left(\frac{2}{\sqrt{t}}\right)dt \\ &= \frac{2\lambda_{SR}\lambda_{RD}\left[\lambda_{RR}(1-\rho)\right]^2}{\kappa^5\Psi^2}\times G_{0,3}^{3,0}\left(\frac{\lambda_{SR}\lambda_{RD}\lambda_{RR}(1-\rho)}{\kappa^2\Psi}\middle|-2,0,0\right).\end{aligned} \tag{30}$$

Finally, substituting (25), (26), (29), and (30) into (20), the EC_{UP} can be given as

$$EC_{UP} = \log_2\left\{\begin{array}{l}1+\dfrac{\lambda_{RR}(1-\rho)}{\kappa^2}\sqrt{\dfrac{\lambda_{SR}\lambda_{RD}\lambda_{RR}(1-\rho)}{\Psi}}G_{0,3}^{3,0}\left(\dfrac{\lambda_{SR}\lambda_{RD}\lambda_{RR}(1-\rho)}{\kappa^2\Psi}\middle|\dfrac{-1}{2},\dfrac{-1}{2},\dfrac{1}{2}\right) \\ \\ +\dfrac{\kappa\Psi}{\lambda_{SR}\lambda_{RD}}-\dfrac{2\lambda_{SR}\lambda_{RD}\left[\lambda_{RR}(1-\rho)\right]^2}{\kappa^5\Psi^2}G_{0,3}^{3,0}\left(\dfrac{\lambda_{SR}\lambda_{RD}\lambda_{RR}(1-\rho)}{\kappa^2\Psi}\middle|-2,0,0\right)\end{array}\right\}. \tag{31}$$

5. Simulation Results

In this section, Monte Carlo simulations [15–21] are conducted to validate the exact and upper bound ergodic capacity derived for the proposed FD DF relaying network with hybrid TSPR. We assume the distances between source to relay and relay to destination equal to the unit value. The means of all the channel gain coefficients $\lambda_{SR}, \lambda_{RR}, \lambda_{RD}$ are equal to 1, the energy harvesting coefficient $\eta = 1$, time-switching factor $\alpha = 0.5$, power-splitting factor $\rho = 0.5$, and Ψ value varies from −5 to 20 dB. The simulation results for the ergodic capacity were achieved by averaging it over 106 random samples for each Rayleigh channel gain.

In Figure 3, the ergodic capacity is presented as a function of Ψ (dB). It is easy to see that when the value of Ψ is less than 4, the EC of hybrid TSPR (HTSPR) outperforms PSR. However, the EC of HTSPR is worse than that of the PSR scheme at a high level of Ψ, i.e., $\Psi > 4$. It is also observed that the TSR scheme always obtains the best performance compared to that of HTSPR and PSR. Furthermore, the increasing Ψ value significantly influences on the EC of the TSR and PSR than the HTSPR scheme. Specifically, when Ψ equals to 20 dB, the HTSPR converses to a saturation value, while the TSP and PSR's EC are still raising. Moreover, the upper bound of the three schemes gives a better EC as compared with the exact ones which are expected.

In Figure 4, we investigate the ergodic capacity as a function of energy harvesting coefficient η for HTPSR scheme with three scenarios: the first scenario with

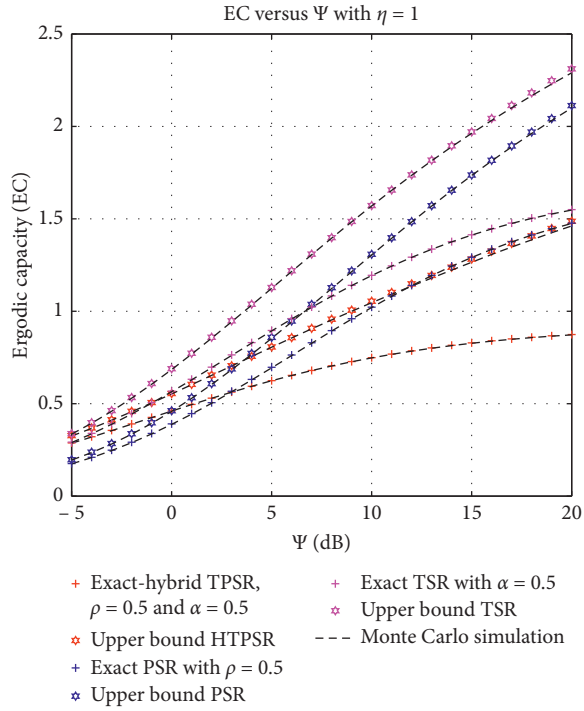

Figure 3: Ergodic capacity versus Ψ.

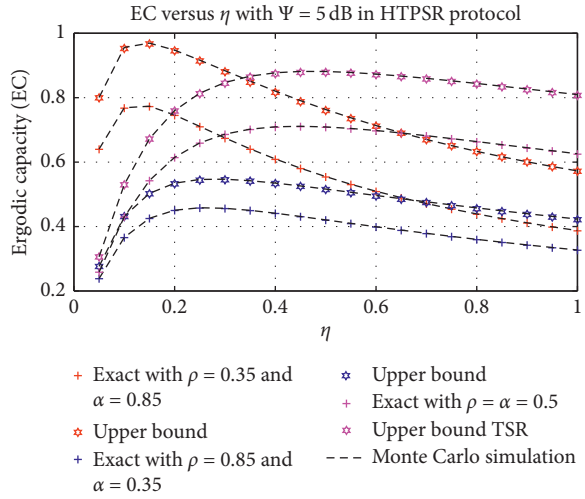

Figure 4: Ergodic capacity versus η for HTPSR protocol.

$\rho = 0.35$ and $\alpha = 0.85$ is called HTPSR1, the second scenario with $\rho = 0.85$ and $\alpha = 0.35$ is called HTPSR2, and the third scenario with $\rho = \alpha = 0.5$ is called HTPSR3. It is shown that the EC of HTPSR protocol obtains a maximum value at an optimal value of energy-efficient coefficient η, and then, it decreases when η increases. Moreover, when the value of the energy-efficient coefficient is less than 0.3, the EC of the HTPSR1 scheme is better than that of other schemes. Nevertheless, when the value of the energy-efficient coefficient is higher than 0.3, the HTPSR1 obtains the best performance, which outperforms others.

In Figure 5, the EC is depicted as a function of α and ρ for the HTPSR scheme, where $\Psi = 1$ and $\eta = 1$. As expected, the EC of the upper bound method is always better than that of the exact one which is verified by the mathematical results. Moreover, Figure 5 shows that there is good agreement between the analysis and the simulation. Because the value of α and ρ significantly influences on the network performance, they impact directly on the allocated time for the EH and information transmission. Consequently, EC can obtain the best value at an optimal α and ρ, and then, the total achievable capacity decreases.

Figures 6 and 7 show the EC as a function of ρ or α for PSR/TSR protocol. The value of ρ or α plays an important role since it influences not only the amount of harvested energy at the relay but also the information transmission

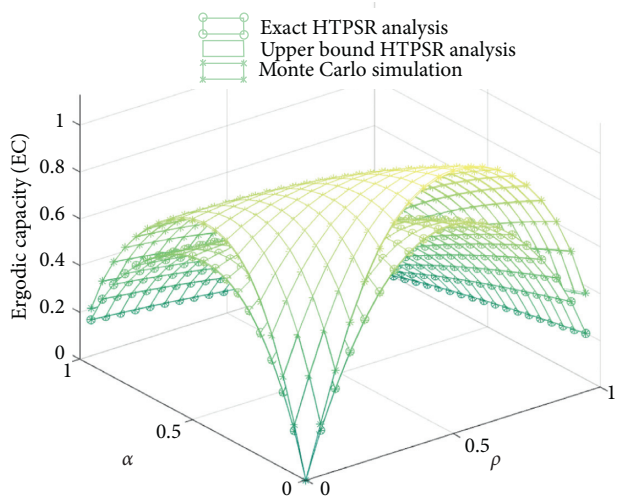

Figure 5: EC versus α and ρ for HTPSR protocol.

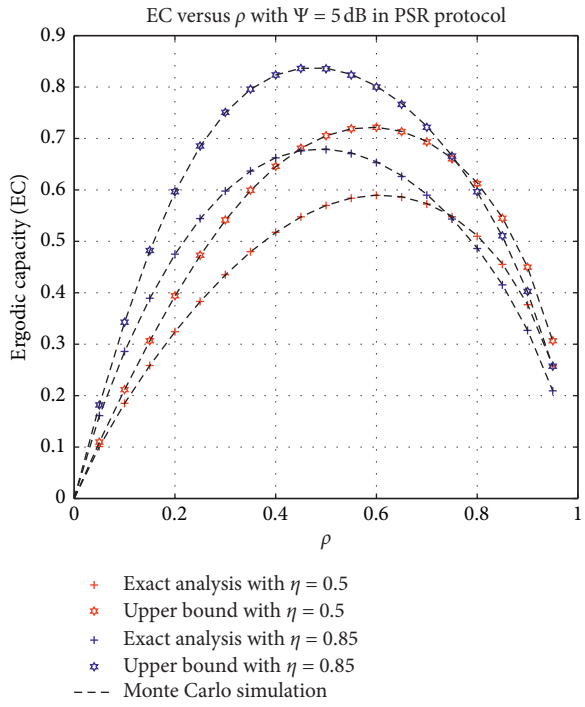

Figure 6: Ergodic capacity versus ρ for PSR protocol.

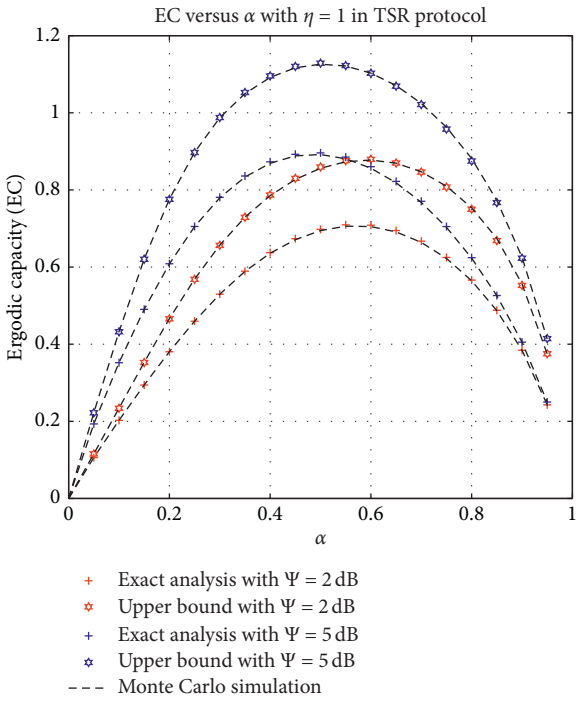

Figure 7: Ergodic capacity versus α for TSR protocol.

from the relay to destination. This can be explained that the higher the value of ρ or α is, the more the energy than the relay can harvest. However, this also means that there is less power/time for information decoding at the destination. It leads to the fact that the ergodic capacity can obtain the maximum value at the optimal point of ρ or α, and the performance decreases. The EC of PSR with $\rho = 0.85$ is better than that of PSR with $\rho =$, 0.5 when $\rho < 0.75$.

Otherwise, when ρ value is bigger than 0.75, the EC of PSR with $\rho =$, 0.85 is worse than that of PSR with $\rho = 0.5$. The same phenomena can be explained as in Figure 7.

6. Conclusions

A new hybrid TPSR protocol for energy harvesting wireless communication networks over DF-based Rayleigh fading channels is proposed and studied in this work. The system model includes one source, one relay, and one destination for data transmission from the source to the destination. We derive the exact and upper bound expressions of the ergodic capacity and then investigate the influence of all designed parameters on the system performance utilizing Monte Carlo simulation. Simulation results show that the hybrid

TPSR can dynamically operate in the TSR or PSR mode by setting ρ or α equal to zero. For future work, the performance analysis can be extended by considering hardware impairment, cognitive radio network, or NOMA.

Data Availability

There are no underlying data supporting the results of our study.

Disclosure

We proposed the model system and performed simulation by Matlab software.

Conflicts of Interest

The authors declare that they have no conflicts of interest.

Authors' Contributions

The main contribution of Phu Tran Tin (phutrantin@iuh.edu.vn) was to execute performance evaluations by theoretical analysis and simulations, while Phan Van-Duc, N. Nguyen Tan (nguyennhattan@tdtu.edu.vn), and Le Anh Vu (leanhvu@tdtu.edu.vn) worked as the advisors of Tan N. Nguyen in discussing, creating, and advising on performance evaluations together.

References

[1] L. R. Varshney, "Transporting information and energy simultaneously," in *Proceedings of the 2008 IEEE International Symposium Information Theory IEEE*, pp. 1612–1616, Ontario Canada, July 2008.

[2] D. H. Tran, T. D. Le, and B. S. Kim, "Stability-aware geographic routing in energy harvesting wireless sensor networks," *Sensors*, vol. 16, pp. 1–15, 2016.

[3] T. P. Tin, B. D. Hoang, N. N. Tan, H. D. Hung, and T. T. Trang, "Power beacon-assisted energy harvesting wireless physical layer cooperative relaying networks: performance analysis," *Symmetry*, vol. 12, no. 1, p. 106, 2020.

[4] H. T. Dinh, T. D. Tran, and B. S. Kim, "Performance enhancement for multi-hop harvest-to-transmit WSNs with path-selection methods in presence of eavesdroppers and hardware noises," *IEEE Sensors Journal*, vol. 18, no. 12, pp. 5173–5186, 2018.

[5] R. Zhang and C. K. Ho, "MIMO broadcasting for simultaneous wireless information and power transfer," *IEEE Transactions on Wireless Communications*, vol. 12, no. 5, pp. 1989–2001, 2013.

[6] T. D. Hieu, G. Sumit, C. Symeon, and O. Bjorn, "Throughput maximization for wireless communication systems with backscatter- and cache-assisted UAV technology," 2020, https://arxiv.org/abs/2011.07955.

[7] P. Grover and A. Sahai, "Shannon meets Tesla: wireless information and power transfer," in *Proceedings of the 2010 IEEE International Symposium on Information Theory*, pp. 2363–2367, Austin, TX, USA, June 2010.

[8] G. Sumit, S. K. Shree, T. D. Hieu, C. Symeon, and O. Bjorn, "Hybrid backscatter and relaying scheme for 6g greencom Iot networks with SWIPT," 2020, https://doi.org/10.36227/techrxiv.12893750.v1.

[9] A. A. Nasir, X. Zhou, S. Durrani, and R. A. Kennedy, "Relaying protocols for wireless energy harvesting and information processing," *IEEE Transactions on Wireless Communications*, vol. 12, no. 7, pp. 3622–3636, 2013.

[10] D. H. Tran, T. D. Tran, and T. D. Le, "Performance evaluation of relay selection schemes in beacon-assisted dual-hop cognitive radio wireless sensor networks under impact of hardware noises," *Sensors*, vol. 18, pp. 1–24, 2018.

[11] N. N. Tan, T. Minh, T. Phuong, and V. Miroslav, "Adaptive energy harvesting relaying protocol for two-way half duplex system network over rician fading channels," *Wireless Communications and Mobile Computing*, vol. 14, pp. 1–11, 2018.

[12] S. Atapattu and J. Evans, "Optimal energy harvesting protocols for wireless relay networks," *IEEE Transactions on Wireless Communications*, vol. 15, no. 8, pp. 5789–5803, 2016.

[13] P. T. Tin, T. N. Nguyen, M. Tran, T. T. Trang, and L. Sevcik, "Exploiting direct link in two-way half-duplex sensor network over block Rayleigh fading channel: upper bound ergodic capacity and exact SER analysis," *Sensors*, vol. 20, no. 4, p. 1165, 2020.

[14] A. Jeffrey and D. Zwillinger, *Table of Integrals, Series, and Products*, Elsevier, Amsterdam, Netherlands, 2015.

[15] N. N. Tan, T. T. Phuong, and V. Miroslav, "Wireless energy harvesting meets receiver diversity: a successful approach for two-way half-duplex relay networks over block rayleigh fading channel," *Computer Networks*, vol. 172, 2020.

[16] N. N. Tan, T. H. Q. Minh, T. T. Phuong et al., "Performance enhancement for energy harvesting based two-way relay protocols in wireless Ad-Hoc networks with partial and full relay selection methods," *Ad-hoc networks*, vol. 45, pp. 178–187, 2019.

[17] H. D. Hung, N. N. Tan, T. Minh, L. Xingwang, T. Phuong, and V. Miroslav, "Security analysis of a two-way half-duplex wireless relaying network using partial relay selection and hybrid TPSR energy harvesting at relay nodes," *IEEE Access*, vol. 13, pp. 187165–187181, 2020.

[18] D. H. Tran, T. D. Tran, and S. G. Choi, "Secrecy performance of a generalized partial relay selection protocol in underlay cognitive networks," *International Journal of Communication Systems*, vol. 31, no. 17, pp. 1–17, 2018.

[19] T. P. Tin, P. D. Van, H. D. Hung, N. N. Tan, T. Minh, and V. Miroslav, "Non-linear energy harvesting based power splitting relaying in full-duplex AF and DF relaying network: system performance analysis," *Proceedings of the Estonian Academy of Sciences*, vol. 12, pp. 368–381, 2020.

[20] D. Le, D. H. Tran, S. Choi, B. Kim, and B. An, "Impact of beamforming on the path connectivity in cognitive radio ad-hoc networks," *Sensors*, vol. 19, 2016.

[21] T. D. Hieu, T. T. Duy, and S. G. Choi, "Performance enhancement for harvest-to-transmit cognitive multi-hop networks with best path selection method under presence of eavesdropper," in *Proceedings of the 2018 20th International Conference on Advanced Communication Technology (ICACT)*, pp. 1-2, Chuncheon-si, Korea (South), August 2018.